

Convergent Cross Mapping (CCM) Notes

January 28, 2014

1 Basic Idea

Convergent cross mapping (CCM) is introduced in *Detecting Causality in Complex Ecosystems*¹ by Sugihara *et. al.*. The supplementary text for that paper is very helpful², although care should be taken when comparing the figure numbers between the text documents (the figure numbers in the supplementary text seem to be off by one).

CCM is a technique used to identify “causality” between time series and is intended to be useful in situations where the only other statistical “causality” measure, Granger causality, is known to be invalid (i.e. in dynamic systems that are “nonseparable”). The authors state that CCM is a “necessary condition for causation”, but it may be best to avoid all discussion of causality in this work. It is well known (refs would be nice) that Granger causality is unrelated to causality as it is typically understood in physics. As such, rather than consider the necessity and sufficiency of CCM for causation, we will use the term “directed correlation”.

CCM is very similar to simplex projection, which was introduced by Sugihara and May in *Nonlinear forecasting as a way of distinguishing chaos from measurement error*³ and *Determining error from chaos in ecological time series*⁴. A concise overview of simplex projection can be found online⁵. Simplex projection uses the points with the most similar histories to the point at t to predict the point at $t + 1$. Similarly, CCM uses points with the most similar histories to a point $X(t)$ (in a time series X) to estimate the point $Y(t)$ (in a time series Y).

2 Algorithm

The algorithm (as it has been implemented here in Matlab) consists of five steps:

1. Create the shadow manifold for X , called M_X
2. Find the nearest neighbours to $X(t)$ in M_X
3. Use the nearest neighbours to create weights
4. Use the weights to estimate $Y(t)$, called $Y(t)|M_X$
5. Find the correlation between $Y(t)$ and $Y(t)|M_X$ (this correlation is what is reported as the “directed correlation”)

The steps vary in complexity and are explained in more detail below.

2.1 Create M_X

Given an embedding dimension E , the shadow manifold of X , called M_X , is created by associating an E -dimensional vector to each point $X(t)$ that is constructed as $\vec{X}(t) = (X(t), X(t-\tau), X(t-2\tau), \dots, X(t-(E-1)\tau))$. The first such vector is created at $t = 1 + (E-1)\tau \equiv t_s$ and the last is at $t = L \equiv t_l$ where L is the time series length (or “library length”). The shadow manifold of X is the collection of all such vectors, i.e. $M_X = \{\vec{X}(t) | t \in [t_s, t_l]\}$. The time step τ is not discussed much in any of the Sugihara papers, and it appears to always be assumed that $\tau = 1$. We will follow that assumption throughout these notes unless specifically stated otherwise.

¹<http://www.uvm.edu/~cdanfort/csc-reading-group/sugihara-causality-science-2012.pdf>

²<http://www.sciencemag.org/content/suppl/2012/09/19/science.1227079.DC1/Sugihara.SM.pdf>

³<http://simplex.ucsd.edu/SugiMay-Chaos.pdf>

⁴<http://simplex.ucsd.edu/SugiGrenMay-Chaos.pdf>

⁵<http://simplex.ucsd.edu/>

2.2 Find Nearest Neighbours

The minimum number of points required for a bounding simplex in an E -dimensional space is $E + 1$ (find a non-Sugihara reference for this statement). Following this requirement, the $E + 1$ nearest neighbours for a point $\vec{X}(t)$ on M_X (remember that this “point” on the shadow manifold is an E -dimensional vector of lagged time series points from X) are found. The distances d to these points and the times t at which they occur are recorded. Thus, the nearest neighbour search results in a set of distances $\{d_1, d_2, \dots, d_{E+1}\}$ and an associated set of times $\{t_1, t_2, \dots, t_{E+1}\}$ (where the subscript 1 denotes the closest neighbour, 2 denotes the next closest neighbour, etc.). The distances for a point $\vec{X}(t)$ are defined as

$$d_i = D(\vec{X}(t), \vec{X}(t_i)) ,$$

where $D(\vec{a}, \vec{b})$ is the Euclidean distance between vectors \vec{a} and \vec{b} (implemented as `norm(a-b)` in the Matlab algorithm).

2.3 Create Weights

Each nearest neighbour will be used to find an associated weight. Define the unnormalized weights as

$$u_i = e^{-\frac{d_i}{d_1}} .$$

In this way, each nearest neighbour will have a set of $E + 1$ weights associated to the distance (and time) sets. The weights are defined as

$$w_i = \frac{u_i}{N} ,$$

where the normalization factor is given as

$$N = \sum_j u_j .$$

2.4 Find $Y(t)|M_X$

A point $Y(t)$ in Y can be estimated using the (normalized) distances to the points in X that have the most similar histories to the point $X(t)$ (i.e. using the weights calculated above). This estimate is calculated as

$$Y(t)|M_X = \sum_i w_i Y(t_i) ,$$

where w_i are the weights calculated in the previous subsection and t_i are the times associated to the nearest neighbours (and, subsequently, the weights w_i).

2.5 Find the Directed Correlation

Define the directed correlation as

$$C_{YX} = \rho_{Y(t), Y(t)|M_X} ,$$

where $\rho_{A,B}$ is the standard Pearson’s correlation coefficient between A and B . It can be seen from the above algorithm that $X = Y \Rightarrow C_{YX} = C_{XY}$, but in general, $C_{YX} \neq C_{XY}$. Consider the following terminology:

- “Directionally correlated from X to Y ” means $C_{YX} < C_{XY}$
- “Directionally correlated from Y to X ” means $C_{YX} > C_{XY}$
- “Bidirectionally correlated from X to Y ” means $C_{YX} = C_{XY}$
- “Uncorrelated from X to Y ” means $C_{YX} = C_{XY} = 0$

The first two terms will be discussed in more detail in the following sections.

3 Point of Confusion

When a system is directionally correlated (called “unilateral causation” by Sugihara *et. al.*) because $X \Rightarrow Y$ (i.e. X “drives” Y), then the system is “directionally correlated from X to Y ”. This language means that X can be estimated from the shadow manifold of Y better than Y can be estimated from the shadow manifold of X . As Sugihara points out, this idea can be confusing. Consider the following quote from the supplementary material:

“This runs counter to intuition (and Granger causality), and suggests that if the weather drives fish populations, we can use fish to predict the weather but not vice versa. Note that CCM does not involve forecasting per se, but predicts (estimates) contemporaneous or past states of causative variables. Thus, if the fish time series contains historical information (in its lags) that allows one to estimate past weather states, this information (the weather information relevant to fish) would be entirely redundant if weather was explicitly added to a model for predicting fish. Thus weather would (incorrectly) not be seen as causative in Granger’s scheme, since it could be added or removed from the model with no effect. Nonseparability arises from the redundant causative information already fully contained in the affected variables (a consequence of Takens’ theorem).”

Intuitively, if X drives Y , then the time series Y contains information about X and (again, intuitively) Y can be predicted from X (if the dynamics are known). This issue illustrates one of the problems with using terminology like “causation” for this method. Notice that this method centers on estimating a value at a time of interest in one time series using points from another time series that have been chosen for their similar histories to the point in that time series at the time of interest. The key idea is comparing histories. If X drives Y , then similar histories of Y will imply similar histories of X (because X drives Y). But notice that it is not necessarily true that similar histories of X will imply similar histories of Y . This idea will be seen in many of the examples below.

To belabour the point, consider the following quote from Parlitz in *Nonlinear Time-Series Analysis*⁶:

“Since the response system “experiences” the dynamics of the drive system it is no surprise that we can use the response time series to predict the drive time series. This is in full agreement with Taken’s theorem. On the other, we can in general not expect that the response time series can be predicted on the basis of the time series from the drive system, because the drive system has no information about the actual dynamics of the response.” [Section 8.9.2]

4 Example System

Consider the example system used by Sugihara *et. al.*:

$$\begin{aligned} X(t) &= X(t-1)(r_x - r_x X(t-1) - \beta_{xy} Y(t-1)) \\ Y(t) &= Y(t-1)(r_y - r_y Y(t-1) - \beta_{yx} X(t-1)) \end{aligned}$$

where $r_x, r_y, \beta_{xy}, \beta_{yx} \in \mathbf{R}$. Even if the four parameters of the systems (i.e. r_x, r_y, β_{xy} and β_{yx}) are set, the CCM analysis of this system depends on three other parameters: the library length L , the embedding dimension E , and the time step τ .

Following Sugihara’s example, let $r_x = 3.8$, $r_y = 3.5$, $\beta_{xy} = 0.01$, and $\beta_{yx} = 0.2$ with the initial conditions of $X(t_0) = 0.4$ and $Y(t_0) = 0.2$. Given this parameter set (and the discussion in the previous section), it is expected that $C_{YX} < C_{XY}$ will be true because $\beta_{yx} > \beta_{xy}$. If $\beta_{yx} > \beta_{xy}$, then X “drives” Y more than Y “drives” X ; hence, the histories of Y will contain more information about X than the histories of X contain about Y , which leads to the aforementioned expectation of $C_{YX} < C_{XY}$. Indeed, $C_{XY} \approx 0.75$ and $C_{YX} \approx -0.11$ for $L = 100$, $E = 2$, and $\tau = 1$.

Notice, however, that the actual values of C_{XY} and C_{YX} depend strongly on L , E , and τ . Figure ?? shows C_{XY} and C_{YX} calculated using all of the parameter values from the previous paragraph but with the library length L ranging from 10 to 500. Both directed correlations appear to converge to some nominal value and $C_{YX} < C_{XY}$ over most of the range (as expected). But, notice that the small library length behaviour does not appear to follow expectations (i.e. $C_{YX} > C_{XY}$ for small L).

If instead the library length is fixed and the embedding dimension is varied, then the behaviour of the directed correlation changes dramatically. Figure ?? shows C_{XY} and C_{YX} calculated using all of the parameter values from above (and with $L = 100$) but with the embedding dimension E ranging from 2 to 50. There are points over the embedding range when $C_{YX} < C_{XY}$ but there are also points where $C_{YX} > C_{XY}$, which is

⁶<http://www.physik3.gwdg.de/~ulli/pdf/P98b.pdf>

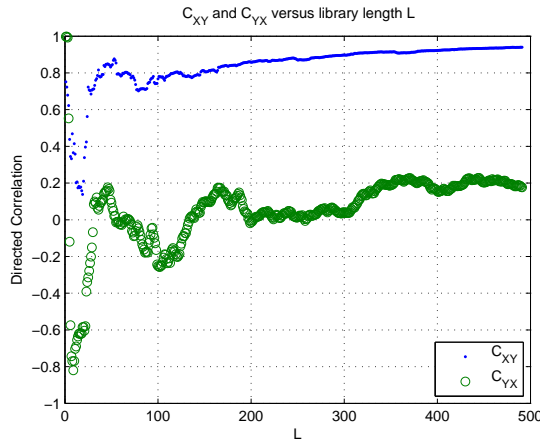
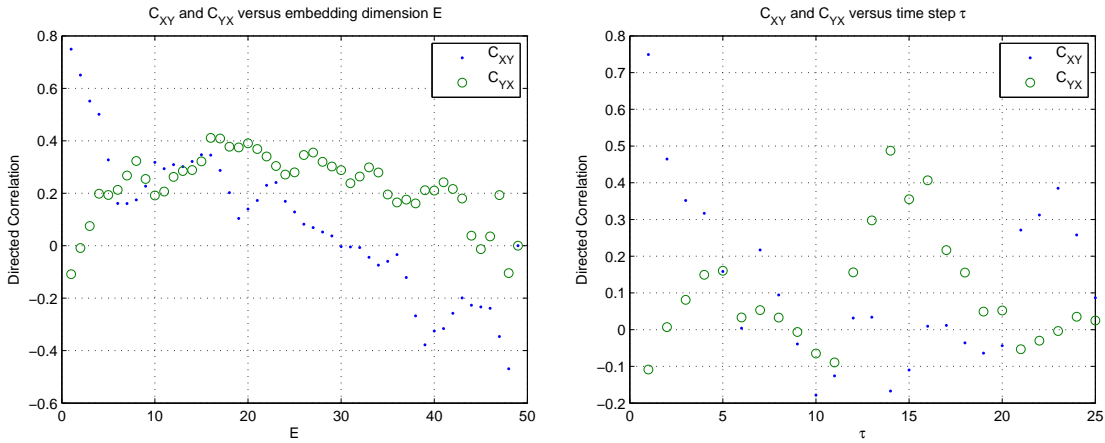


Figure 1: $(r_x, r_y, \beta_{xy}, \beta_{yx}, X(t_0), Y(t_0)) = (3.8, 3.5, 0.01, 0.2, 0.4, 0.2)$ with $\tau = 1$ and $E = 2$.

difficult to interpret with the given parameter set. The dependence on the embedding dimension is concerning because it implies that incorrect conclusions can be drawn about natural data sets (i.e. time series where the theoretical dynamics are not known) regarding which directed correlation is dominate (i.e. which time series is the dominate “driver”). Similar issues arise when plotting the directed correlation over a range for the time step τ from 1 to 25 (see Figure ??).



(a) $(r_x, r_y, \beta_{xy}, \beta_{yx}, X(t_0), Y(t_0)) = (3.8, 3.5, 0.01, 0.2, 0.4, 0.2)$ with $\tau = 1$ and $L = 100$. (b) $(r_x, r_y, \beta_{xy}, \beta_{yx}, X(t_0), Y(t_0)) = (3.8, 3.5, 0.01, 0.2, 0.4, 0.2)$ with $E = 2$ and $L = 100$.

Figure 2

The directed correlation acts as expected for $L = 100$, $E = 2$, and $\tau = 1$. These values can be used (along with r_x and r_y) to see how the directed correlation behaves over a range of β_{yx} given $\beta_{xy} = 0.5$. Figure ?? shows C_{YX} and C_{XY} plotted over the range $\beta_{yx} \in [0.01, 1.0]$ (with $\beta_{xy} = 0.5$), and Figure ?? shows the difference $\Delta = (C_{XY} - C_{YX})$ over the same range. Notice that Δ is an increasing function of β_{yx} that crosses zero around $\beta_{yx} = 0.5$, as expected given the discussion of the CCM algorithm in the beginning sections. Figure ?? is a plot of Δ of ranges for both coupling constants, i.e. $\beta_{xy} \in [0.01, 1.0]$ and $\beta_{yx} \in [0.01, 1.0]$. Following the intuitive expectation, $\beta_{xy} > \beta_{yx} \Rightarrow \Delta < 0$ and $\beta_{xy} < \beta_{yx} \Rightarrow \Delta > 0$.

Notice, Δ is not symmetric about zero for the pair (β_{xy}, β_{yx}) ; i.e.

$$(\beta_{xy}, \beta_{yx}) = (0.5, 0.01) \Rightarrow \Delta \approx -0.27 ,$$

but

$$(\beta_{xy}, \beta_{yx}) = (0.01, 0.5) \Rightarrow \Delta \approx 0.42$$

which is positive but not 0.27. The difference Δ is symmetric about zero given the entire parameter set for each time series, i.e.

$$(r_x, r_y, \beta_{xy}, \beta_{yx}, X(t_0), Y(t_0)) = (3.8, 3.5, 0.5, 0.01, 0.4, 0.2) \Rightarrow \Delta \approx -0.27$$

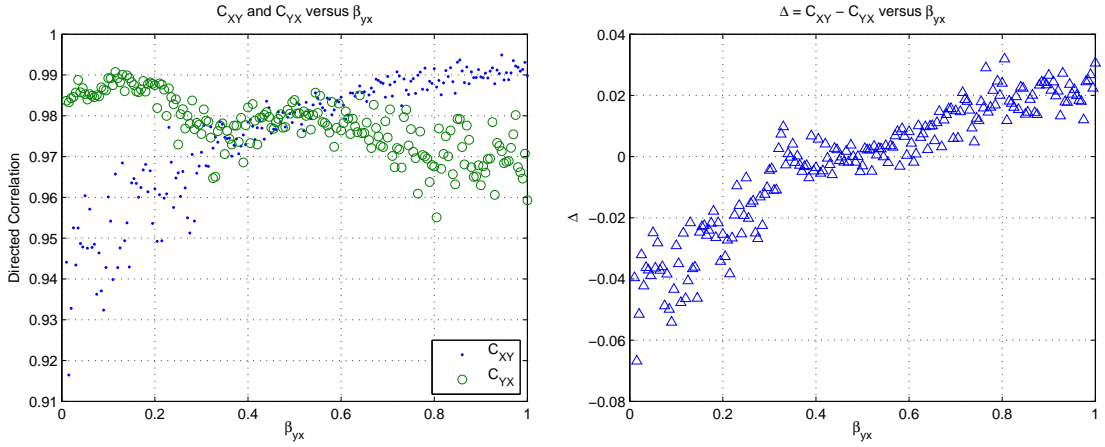


Figure 3

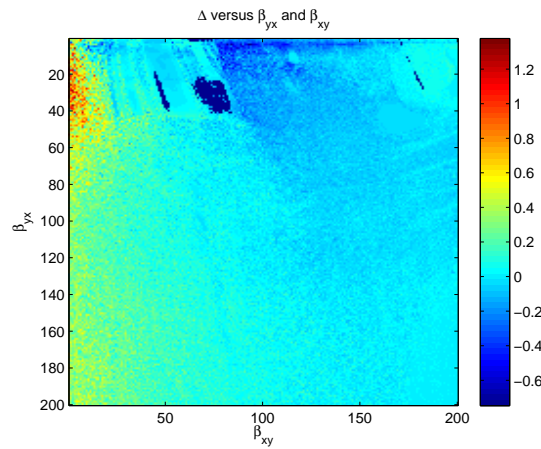


Figure 4: $(r_x, r_y, X(t_0), Y(t_0)) = (3.8, 3.5, 0.2, 0.4, 0.2)$ with $(E, L, \tau) = (2, 100, 1)$.

and

$$(r_x, r_y, \beta_{xy}, \beta_{yx}, X(t_0), Y(t_0)) = (3.5, 3.8, 0.01, 0.5, 0.2, 0.4) \Rightarrow \Delta \approx 0.27 .$$

Given the results of this section, the CCM algorithm does provide a kind of coarse grained quantification of the idea of “driving” between two time series. More specifically, the sign of Δ provides information about the relative strength of dependencies between two time series.

5 Embedding Dimension and Lag Time Step

The embedding dimension (E) dependence of the CCM algorithm in the above examples implies a strong need to understand that dependence in terms of the time series used to create the shadow manifold. It would be difficult to justify any results derived from the use of the CCM method on empirical data (e.g. the solar data) without such an understanding. The ideal solution would be the development of simple statistical procedures (e.g. through the use of autocorrelations, entropies, etc.) to find the “correct” embedding dimension E_X given a times series X .

Consider the Sugihara example system with $(r_x, r_y, \beta_{xy}, \beta_{yx}, X(t_0), Y(t_0)) = (3.8, 3.5, 0.01, 0.2, 0.4, 0.2)$. Define the l -lagged autocorrelation A_l^X of $X(t)$ as $A_l^X = \rho_{X(t), X(t-l)}$ given $t \in (l, L]$ where L is the library length. For this example system, both $|A_l^X|$ and $|A_l^Y|$ can be plotted as a function of l . See Figure ???. The max and min of $|A_l^X|$ occur at $l = 1$ and $l = 21$, respectively, and the max and min of $|A_l^Y|$ occur at $l = 1$ and $l = 30$. Define $\Delta = C_{XY} - C_{YX}$. Given the parameters of this example system, it is expected that $\Delta > 0$ (because “intuitively”, the parameter set seems to imply $X \Rightarrow Y$ for this example). The embedding dimension dependence of Δ can be plotted to reiterate the conclusions of the previous section. See Figure ???. Notice $\Delta = \max_E \Delta$ for $E = 2$ which corresponds a autocorrelation lag $l = 1$. So, it appears that for this example system, the required embedding dimension E to achieve $\Delta = \max_E \Delta$ could be found by determining l such

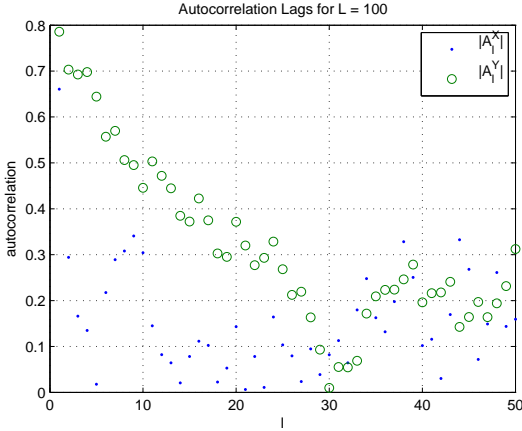
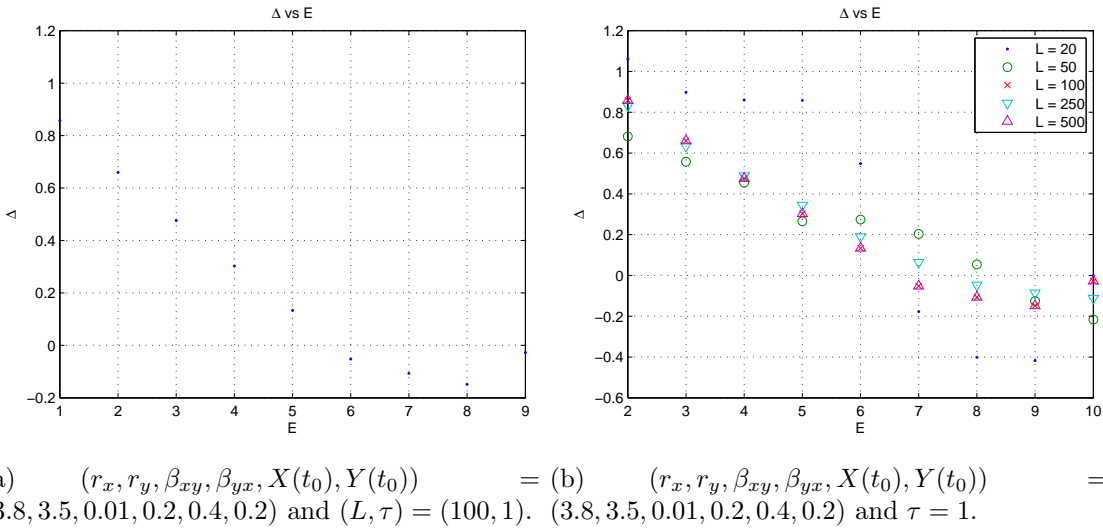


Figure 5: $(r_x, r_y, \beta_{xy}, \beta_{yx}, X(t_0), Y(t_0)) = (3.8, 3.5, 0.01, 0.2, 0.4, 0.2)$.



(a) $(r_x, r_y, \beta_{xy}, \beta_{yx}, X(t_0), Y(t_0)) = (3.8, 3.5, 0.01, 0.2, 0.4, 0.2)$ and $(L, \tau) = (100, 1)$. (b) $(r_x, r_y, \beta_{xy}, \beta_{yx}, X(t_0), Y(t_0)) = (3.8, 3.5, 0.01, 0.2, 0.4, 0.2)$ and $\tau = 1$.

Figure 6

that $|A_l^X| = \max_l |A_l^X|$ and $|A_l^Y| = \max_l |A_l^Y|$. However, it can be seen from the plot that $E \in [2, 5] \rightarrow \Delta > 0$ and $E \in [6, 10] \rightarrow \Delta < 0$. This change in sign of Δ does not appear to correlate with the autocorrelation lags in a straightforward way akin to the above relationship between l and $\max_E \Delta$. The lack of correlation between l and the positivity of Δ may indicate the the relationship between l and $\max_E \Delta$ is coincidental or a specific property of this example system. Also notice the value of E for which Δ changes signs depends on the library length L (although, for this example at least, the value of E such that $\Delta = \max_E \Delta$ seems to be independent of L). See Figure ?? to see the data that leads to this observation. Before these ideas are explored with other example systems, consider the question of why E is the same for both shadow manifolds.

There does not seem to be any *a priori* reason that E needs to be the same for both shadow manifolds used to calculate Δ . Figure ?? shows Δ as a function of the embedding dimension used to create the X shadow manifold, E_X , and the embedding dimension used to create the Y shadow manifold, E_Y . Notice that $E_X \in [2, 4] \rightarrow \Delta > 0 \forall E_Y \in [2, 10]$ and $E_Y \in [2, 6] \rightarrow \Delta > 0 \forall E_X \in [2, 10]$. So, at least for this example system and embedding dimensions $\in [2, 10]$, achieving $\Delta > 0$ is not necessarily dependent on both E_X and E_Y .

Consider the Sugihara example system with $(r_x, r_y, \beta_{xy}, \beta_{yx}, X(t_0), Y(t_0)) = (3.1, 3.9, 0.2, 0.002, 0.4, 0.2)$. This parameter set leads to the expectation of $\Delta < 0$ and, indeed, $\Delta < 0$ if $(L, \tau) = (100, 1)$ with $E_X, E_Y \in [2, 3]$. See Figure ???. Plotting $|A_l^X|$ and $|A_l^Y|$ for this example system (see Figure ??) reveals $|A_l^X| = \max_l |A_l^X|$ and $|A_l^Y| = \max_l |A_l^Y|$ for $l = 1$, just as in the example of the previous paragraphs. So, the above method to determine the “correct” embedding dimension from the data using autocorrelation lags seems to provide answers that agree with intuition in at least two examples. Although it should be noted that in the second example, preserving the intuitive conclusion (i.e. $\Delta < 0$) cannot be achieved with $E_X = 2$ with any $E_Y \in [2, 10]$ or E_Y with any $E_X \in [2, 10]$. In constraint to the first example, it is possible in the second example to achieve $\Delta > 0$ with $E_{X(Y)} = 2$ and $E_{Y(X)} \in [6, 10]$.

The shadow manifold is used to estimate the time series of interest, so it seems reasonable that the em-

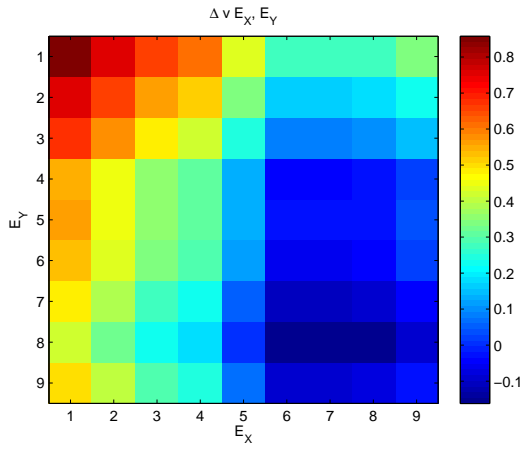
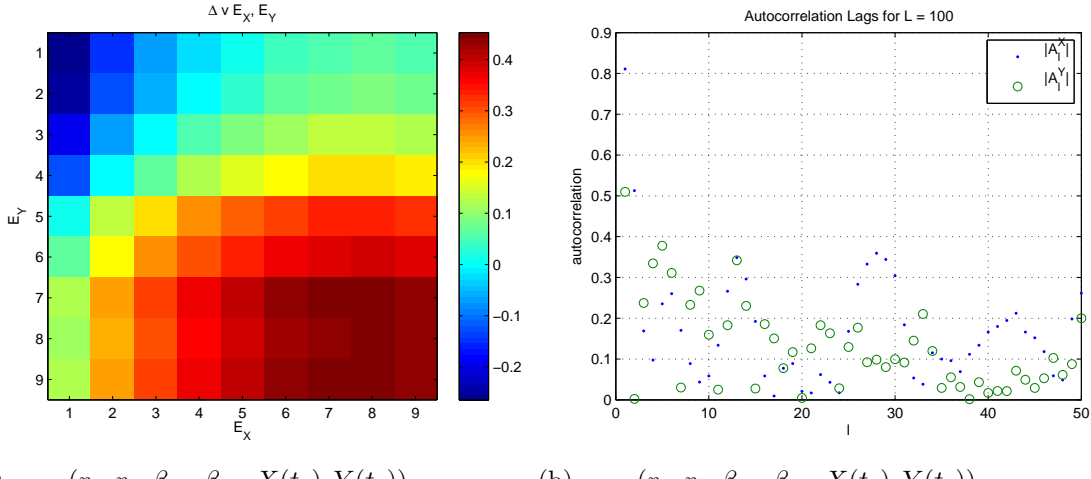


Figure 7: $(r_x, r_y, \beta_{xy}, \beta_{yx}, X(t_0), Y(t_0)) = (3.8, 3.5, 0.01, 0.2, 0.4, 0.2)$ and $(L, \tau) = (100, 1)$.



(a) $(r_x, r_y, \beta_{xy}, \beta_{yx}, X(t_0), Y(t_0)) = (3.1, 3.9, 0.2, 0.002, 0.4, 0.2)$ and $(L, \tau) = (100, 1)$. (b) $(r_x, r_y, \beta_{xy}, \beta_{yx}, X(t_0), Y(t_0)) = (3.1, 3.9, 0.2, 0.002, 0.4, 0.2)$ and $(L, \tau) = (100, 1)$.

Figure 8

bedding dimension of the shadow manifold should be related to the autocorrelation lag of the time series of interest rather than the times series used to create the shadow manifold. Notice that this approach would not change the relationship between l and $\max_E \Delta$ discussed in the previous paragraph.

Using the autocorrelation method discussed above may provided embedding dimensions that agree with intuition, but the method does not explain the apparent dependence of the CCM on embedding dimension. As an attempt o understand this dependence consider the following algorithm (“NN1”):

1. Embed X in a manifold with dimension E .
2. Record the time step locations \tilde{t}_i^E (in the original X) and weights w_i^E of the $N = E + 1$ dimensional point $X(t)$
3. Repeat steps 1 and 2 for $E = E + 1$.
4. Stop when $\{\tilde{t}_i^E\} \neq \{\tilde{t}_i^{E-1}\}$; i.e. stop when the set of time step locations in the N -dimensional point given E is not the same as the set of time step locations in the N -dimensional point given $E - 1$. (Notice that the algortihm completely ignores $\{w_i^E\}$.)
5. Record E (i.e. the embedding dimension for which the above iteration is halted) as E_t^H .
6. Repeat steps 1-4 for $t = t + 1$ for all $t \leq T$ where T is dependent on the library length L of X .
7. Find the mode of $\{E_t^H\}$.

Also consider the following, very similar, algorithm (“NN2”):

1. Embed X in a manifold with dimension E .

2. Record the time step locations \tilde{t}_i^E (in the original X) and weights w_i^E of the $N = E + 1$ dimensional point $X(t)$
3. Repeat steps 1 and 2 for $E = E + 1$.
4. Stop when $\exists w_i^E < \delta$; i.e. stop when one of the weights N -dimensional point drops below some cutoff value δ . (Notice that the algorithm completely ignores $\{\tilde{t}_i^E\}$.)
5. Record E (i.e. the embedding dimension for which the above iteration is halted) as E_t^H .
6. Repeat steps 1-4 for $t = t + 1$ for all $t \leq T$ where T is dependent on the library length L of X .
7. Find the mode of $\{E_t^H\}$.

The second algorithm (NN2) requires the selection of some δ and both algorithms require determining T . Consider the Sugihara example with $(r_x, r_y, \beta_{xy}, \beta_{yx}, X(t_0), Y(t_0)) = (3.8, 3.5, 0.01, 0.2, 0.4, 0.2)$ and $(L, \tau) = (100, 1)$. Applying NN1 to X yields 7 for $T \in [1, 50]$. Applying NN2 to X with $T = 10$ yields 2 for $\delta = 0.05$ and $\delta = 0.01$. The addition of the free parameter δ makes NN2 a little less convincing than NN1 (e.g. how is a particular choice for δ justified?). The behaviour of NN2 on X for $T \in [1, 50]$ and $\delta \in [10^{-5}, 10^{-2}]$ (in steps of ??) can be seen in ??.

It might be assumed that the dependence of Δ on E implies a similar dependence of Δ on the lagged time step τ because of (co-dependent?) roles E and τ play in the construction of the shadow manifold. To explore these idea, introduce τ_X and τ_Y in analogy to E_X and E_Y . Figures ?? and ?? show Δ does have a dependency on $\tau_{X(Y)}$ and, like $E_{X(Y)}$, leads to “unintuitive” results for large τ . To reinforce the idea, Figures ?? and ??

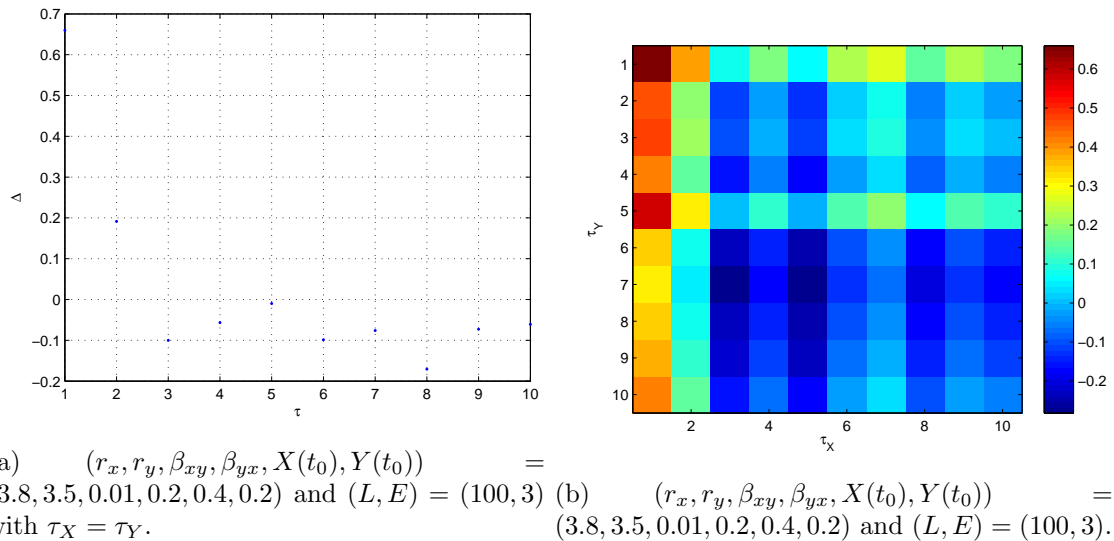


Figure 9

show similar results for the Sugihara system with the coefficients used to produce Figure fig:SugEx2VaryE. Notice that both examples lead to unintuitive results much quicker as $\tau_{X(Y)}$ is increased than when $E_{X(Y)}$ was increased. This apparent larger sensitivity of the CCM algorithm on τ than E implies that care must be taken to carefully choose both. The autocorrelation method proposed above to find E also works to find the lagged time step τ with the largest intuitive results; i.e. $|A_l^X| = \max_l |A_l^X|$ and $|A_l^Y| = \max_l |A_l^Y|$ for $l = 1$ (for both examples discussed in this paragraph) and $\Delta = \max_\tau \Delta$ for $\tau = 1$ with $\tau_{X(Y)} = 1$ (again, for both examples). Hence, the autocorrelation method may be a good option for determining $\tau_{X(Y)}$.

As expected, there is also a co-dependence of Δ on E and τ if both are changed simultaneously, as seen in Figures ?? and ?? for both examples discussed in the previous paragraphs. This co-dependence complicates the use of an algorithm like NN1 or NN2 to determine E (or τ) because of the use of the points in the shadow manifold (which depends on both parameter, rather than just the one parameter being iterated). This shortcoming can be overcome by extending NN1 (or NN2) to include iterations over both parameters (e.g. called NN1_{ex} or NN2_{ex} to effectively search the entire 2D parameter space of (E, τ) and applying exactly the same logic as used in the original NN1 (or NN2) algorithm. Unfortunately, the changes necessary to NN1(2) to create NN1(2)_{ex} introduce a computational load that would make the algorithms difficult to apply to large datasets (like the solar data). As such, the autocorrelation method (which is independent of the shadow

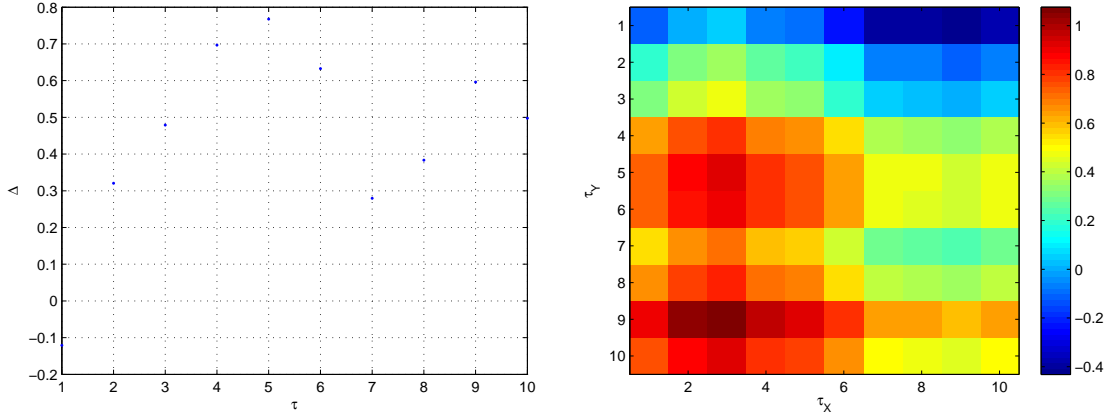


Figure 10

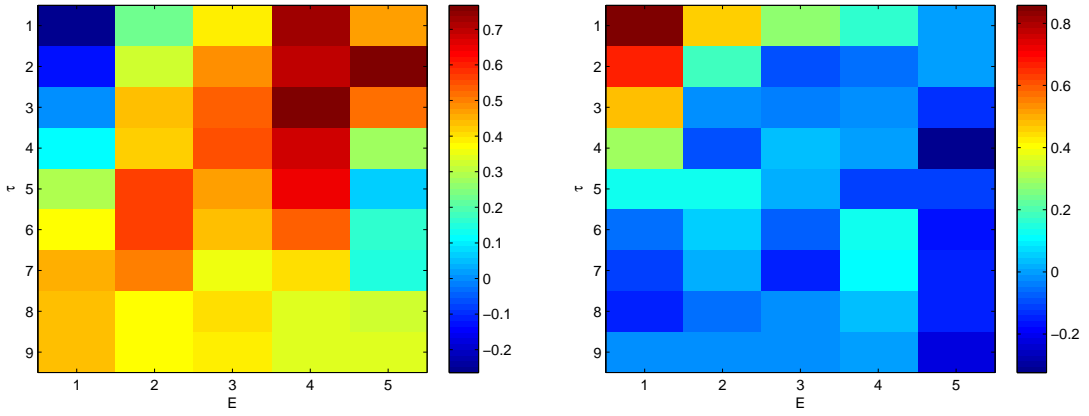


Figure 11

manifold) can be used to set the lagged time step τ and then NN1 (or NN2) can be used to determine E . This two step process to determine “reasonable” parameters for the CCM algorithm will be explored outside of the Sugihara example in the next section.

As a final note, notice that the “intuitive/unintuitive result” cutoff (let’s call this c_u so I can stop writing “intuitive”) depends not only on E and τ (as was shown above) but also on the parameters of the system itself. This complicated behaviour of c_u makes it frustrating (perhaps impossible?) to understand it in terms of the CCM algorithm parameters alone. As an illustration of this point, set $(r_x, r_y, \beta_{xy}, X(t_0), Y(t_0)) = (3.8, 3.5, 0.01, 0.4, 0.2)$ and $(L, \tau) = (100, 1)$ where $\tau_X = \tau_Y = \tau$. Plotting Δ versus $E = E_X = E_Y$ for different values of β_{yx} reveals that c_u varies with β_{yx} (see Figure ??). Given the dynamics of the Sugihara example it would seem, if everything else is kept constant, that X is a stronger driver of Y as β_{yx} increases. Unfortunately, such “intuition” is not seen in the resulting figure. Notice $\beta_{yx} = 10^{-4}$ (which obeys $\beta_{yx} < \beta_{xy}$) leads to no c_u with the plotted range of $E \in [2, 10]$. The other plotted values of β_{yx} show a wide variety of c_u that have no obvious relationship to each other. It is hard to have confidence in the application of the CCM method to measured data sets when this type of behaviour is so difficult to understand even in example systems.

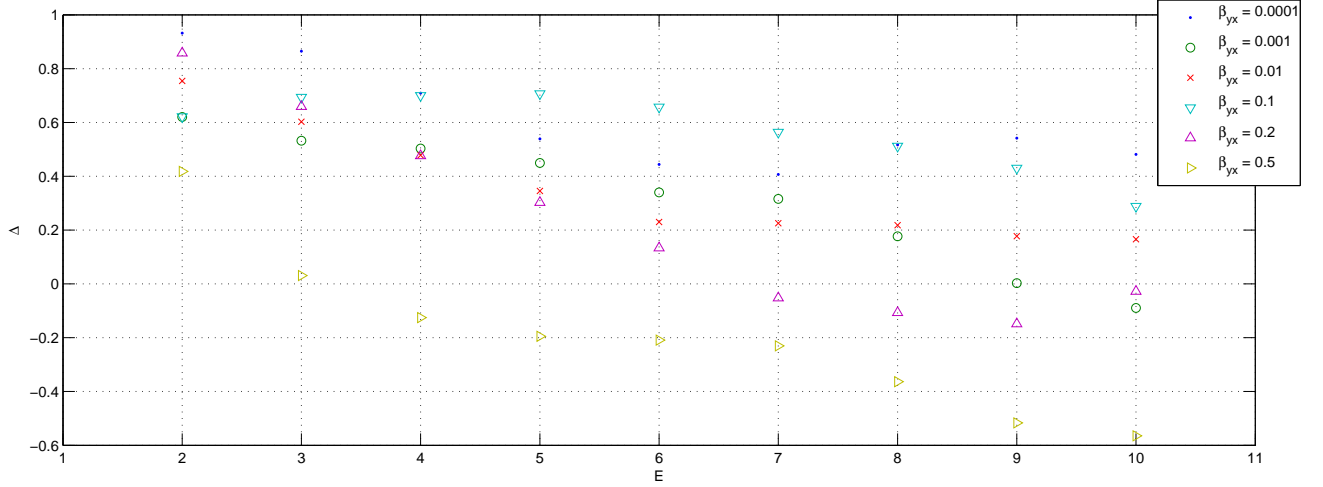


Figure 12: $(r_x, r_y, \beta_{xy}, X(t_0), Y(t_0)) = (3.8, 3.5, 0.01, 0.4, 0.2)$ and $(L, \tau) = (100, 1)$ where $\tau_X = \tau_Y = \tau$ and $E_X = E_Y$.

6 Sampling the Two Population Dynamics (Sugihara Example)

The two-population dynamical system used Sugihara *et. al.*,

$$\begin{aligned} X(t) &= X(t-1)(r_x - r_x X(t-1) - \beta_{xy} Y(t-1)) \\ Y(t) &= Y(t-1)(r_y - r_y Y(t-1) - \beta_{yx} X(t-1)) \end{aligned}$$

where $r_x, r_y, \beta_{xy}, \beta_{yx} \in \mathbf{R}$, is very sensitive both the initial condition $X(t_0)$ and $Y(t_0)$ but also the dynamics parameters r_x, r_y, β_{xy} , and β_{yx} . Consider the following table of values for X and Y :

	$X(t) = -1$	$X(t) = 0$	$X(t) = 1$
$Y(t) = -1$	$(-2r_x - \beta_{xy}, -2r_y - \beta_{yx})$	$(0, -2r_y)$	$(\beta_{xy}, \beta_{yx} - 2r_y)$
$Y(t) = 0$	$(-2r_x, 0)$	$(0, 0)$	$(0, 0)$
$Y(t) = 1$	$(\beta_{xy} - 2r_x, \beta_{yx})$	$(0, 0)$	$(-\beta_{xy}, -\beta_{yx})$

Table 1: The entries are $(X(t+1), Y(t+1))$.

The points $X(t) = 0$ and $Y(t) = 0$ are fixed points for this system. The change in X (or Y) can be derived as follows:

$$X(t) - X(t-1) = r_x \left(X(t-1) - (X(t-1))^2 - X(t-2) + (X(t-2))^2 \right) + \beta_{xy} (X(t-2)Y(t-2) - X(t-1)Y(t-1)) \quad (1)$$

Let $\delta_t = X(t) - X(t-1)$. The above equation can then be rewritten as

$$\delta_t = \delta_{t-1} r_x (1 - X(t-1) - X(t-2)) + \beta_{xy} (X(t-2)Y(t-2) - X(t-1)Y(t-1)) \quad (2)$$

The parameters r_x and r_y can, as seen in the above equation, can lead to rapid growth of the time series to infinity (it is assumed that β_{xy} and β_{yx} are fixed). The change between steps t and $t-1$ depends on r_x times the change between steps $t-1$ and $t-2$; i.e. a large r_x can lead to a rapid growth in the change of X between time steps. As such, the parameters need to be carefully set to insure an oscillating system, which is our desire when testing the CCM algorithm.

All of the previous results using this Sugihara example used fixed values for r_x, r_y, β_{yx} , and β_{xy} with fixed initial conditions $X(t_0)$ and $Y(t_0)$. These values can be sampled (from some reasonable distribution) to investigate the “robustness” of the directed correlation concept. More specifically, if the directed correlation is assumed to have a “reasonable” interpretation related to the coupling in the dynamics (i.e. β_{yx} and β_{xy}), then varying the initial conditions and dynamics parameters (i.e. r_x and r_y) should still lead to “intuitive” results.

The initial conditions will be sampled from normal distributions with means μ_{x0} and μ_{y0} and variances σ_{x0}^2 and σ_{y0}^2 . Likewise, the dynamics parameters will be sampled from normal distributions with means μ_{rx}

and μ_{ry} and variances σ_{rx}^2 and σ_{ry}^2 . The CCM algorithm parameters E (embedding dimension) and τ (lag time step) will be set to 3 and 1, respectively, following the discussion of the previous section. Of course, that still leaves the algorithm parameter of library length for this example (i.e. the time series is created computationally using the two-population dynamics model, so the library length is only limited by practical concerns of computational resources). Figure ?? reveals the same dependence on library length seen in the previous section with $\beta_{xy} = 0.02$ and $\beta_{yx} = 0.1$.

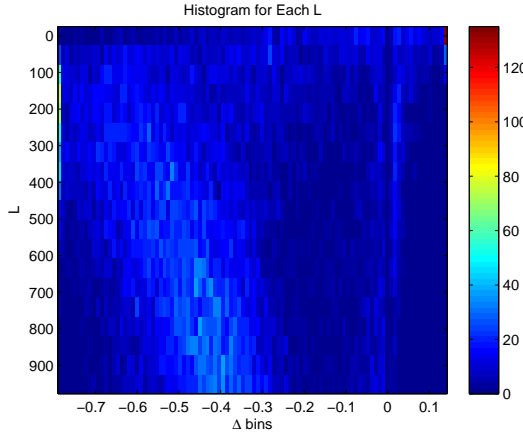


Figure 13: 1000 samples with $(\mu_{rx}, \mu_{ry}, \sigma_{rx}^2, \sigma_{ry}^2, \mu_{x0}, \mu_{y0}, \sigma_{x0}^2, \sigma_{y0}^2) = (3.8, 3.5, 0.1, 0.1, 0.4, 0.2, 0.3, 0.3)$ and $(E, \tau) = (3, 1)$ for $L = 51, 101, 151, \dots, 1000$ with “zeroes removed” (see text for a discussion of zero removal).

Notice that there are dynamic parameter combination that occur within this sample space (as defined in the previous paragraph) with non-negligible probability that cause the dynamical system to (rapidly) diverge (i.e. $X(t) \rightarrow \pm\infty$ and $Y(t) \rightarrow \pm\infty$ as $t \rightarrow \infty$) or reach a fixed point as described above. For example, $(r_x, r_y, X(t_0), Y(t_0)) = (4.04, 3.39, 7.31x10^{-2}, 4.94x10^{-2})$ and $(r_x, r_y, X(t_0), Y(t_0)) = (3.85, 3.49, 1.00, 4.56x10^{-1})$ cause the system to diverge and occurred within a 100 samples given the sampling parameters of $(\mu_{rx}, \mu_{ry}, \sigma_{rx}^2, \sigma_{ry}^2, \mu_{x0}, \mu_{y0}, \sigma_{x0}^2, \sigma_{y0}^2) = (3.8, 3.5, 0.1, 0.1, 0.4, 0.2, 0.3, 0.3)$ with $L = 100$. Such dynamic parameter sets are not interesting to this analysis because it is assumed that the system does not diverge, and such concerns will not be present in empirical data sets. As such, sample with divergent directed correlations will be discarded from the sample set. Notice that $\Delta = 0$ does not necessarily imply diverge time series or vanishing directed correlations (despite the way the data appears in Matlab), so care must be taken in identifying which sample points to discard. Discarding sample in this fashion will be referred to as “removing zeroes” and data sets that have result from such a procedure will be said to have had “zeroes removed”.

Figure ?? shows 3000 samples of the 2-population dynamical system that was sampled in the manner described above with coupling constants of $\beta_{xy} = 0.02$ and $\beta_{yx} = 0.1$. These parameters lead to an expectation of $\Delta < 0$. The figure shows a dominant peak at $\Delta < 0$ but it also shows a secondary peak around $\Delta = 0$. Figure ?? shows that these peaks are still present after 10000 samples. Taking the sample mean would lead to a directed correlation that agrees with intuition, but the second peak about zero is slightly confusing. Figure ?? shows a set of dynamic parameters and coupling constants expected to lead to $\Delta > 0$. Again, the sample mean and histogram after 3000 samples agrees with intuition, but there is still a secondary peak about $\Delta = 0$. Figure ?? shows that setting the mean and variances of the sampling distribution equal for both the initial condition and the dynamic parameter r will lead to a sharp peak about zero (5000 samples) even if the coupling constants are unequal. This result implies that the secondary peak seen in the other plots results from samples where the dynamic parameter sets yield $r_x \approx r_y$ and $X(t_0) \approx Y(T_0)$. This behaviour of the 2-population dynamical system is interesting but does not seem to reveal a shortcoming of the directed correlation approach (rather it appears to be an interesting feature of a specific dynamical system). Notice that dynamic parameter sets that are equal can still lead to $\Delta = 0$ even if the coupling constants are different from each other. This effect can explain the second peak about $\Delta = 0$ in the above histograms. Figure ?? shows that equal dynamic parameter set for X and Y can lead to $X(t)$ and $Y(t)$ being nearly identical. The shadow manifold generated with X would likewise be nearly identical the shadow manifold generated by Y and the CCM correlations would be equal (which leads to $\Delta = 0$ as seen above).

The coupling constants can be varied and the sample means can be plotted as a function of those coupling constants to reveal that the sample means do in fact follow intuition. That plot is Figure ??.

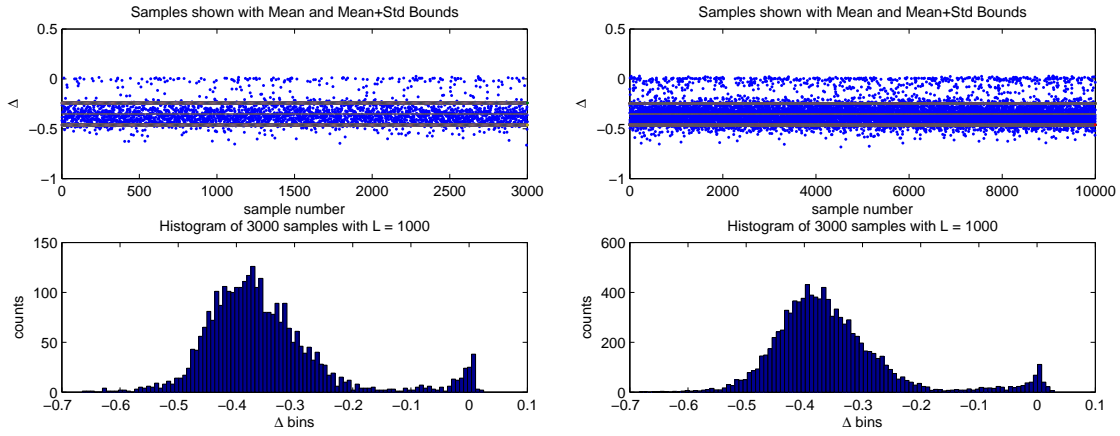


Figure 14

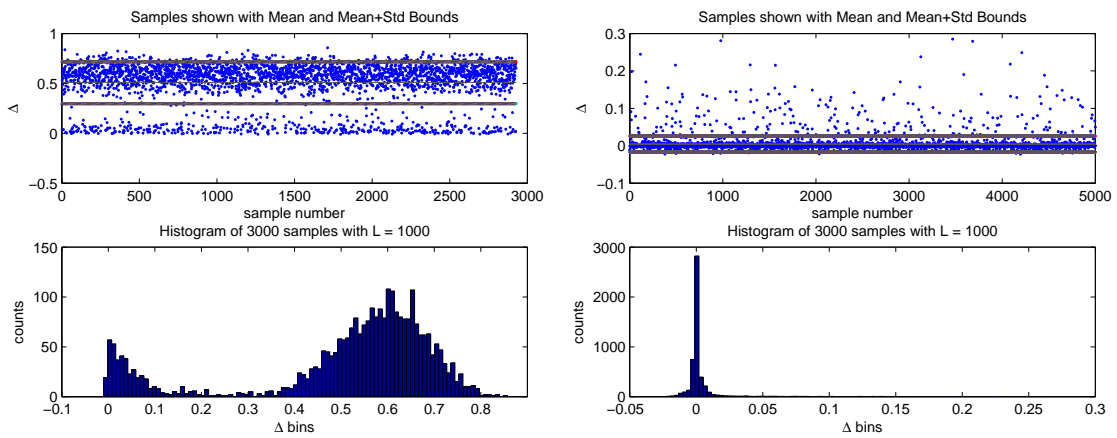


Figure 15

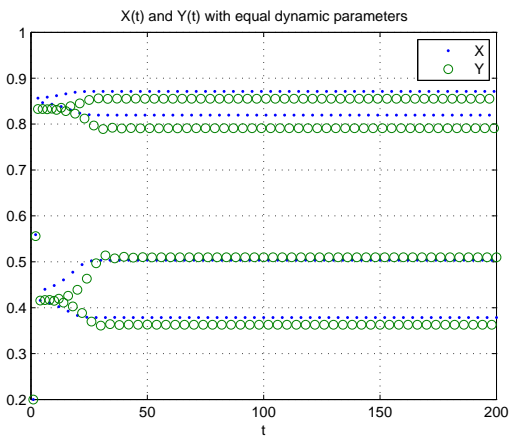


Figure 16: X and Y versus time with $(\mu_{rx}, \mu_{ry}, \sigma_{rx}^2, \sigma_{ry}^2, \mu_{x0}, \mu_{y0}, \sigma_{x0}^2, \sigma_{y0}^2) = (3.5, 3.5, 0.1, 0.1, 0.2, 0.2, 0.3, 0.3)$ and $(E, \tau) = (3, 1)$ for $L = 1000$.

Figure 17: ?? samples at each point with $(\mu_{rx}, \mu_{ry}, \sigma_{rx}^2, \sigma_{ry}^2, \mu_{x0}, \mu_{y0}, \sigma_{x0}^2, \sigma_{y0}^2) = (3.8, 3.5, 0.1, 0.1, 0.4, 0.2, 0.3, 0.3)$ and $(E, \tau) = (3, 1)$ for $L = ??$ with “zeroes removed” (see text for a discussion of zero removal) over the range $\beta_{xy}, \beta_{yx} \in [0, 1]$ in steps of 0.01.

7 Directed Correlation Defined Geometrically

The directed correlation is defined above as a difference of the two cross convergent mapping (CCM) correlations. The CCM correlations ρ_{XY} are defined as the square of the correlation coefficient between a time series X and its CCM-generated counterpart $X|Y$ (i.e. X generated using the “shadow manifold” of a second times series Y). The directed correlation Δ was written above as

$$\Delta \equiv \rho_{XY} - \rho_{YX} ,$$

and the sign of Δ was used to indicate the “driving” time series (i.e. $\Delta > 0 \rightarrow "X \text{ drives } Y"$, $\Delta < 0 \rightarrow "Y \text{ drives } X"$, and $\Delta = 0$ indicates no directed correlation in the system).

Notice $\rho_{XY} \in [0, 1] \rightarrow \Delta \in [-2, 2]$. The bound $\Delta \in [0, 1]$ can be accomplished with $\Delta = \Delta'$ where

$$\Delta' = \frac{1}{2} \left(\frac{\Delta}{2} + 1 \right) ,$$

but such a normalization may make the data analysis even more confusing. The new Δ would obey the same “driving” rules as the one above with 0 replaced with 1/2. The problem with this definition for the directed correlation is not the bounds. Rather, the problem is that this definition may hide information in the CCM correlations that may be of some use. For example, (using the “new” definition) $\Delta = 0.5025$ could result from either $\rho_{XY} = 0.99$ and $\rho_{YX} = 0.98$ or $\rho_{XY} = 0.06$ and $\rho_{YX} = 0.05$. These two different sets of CCM correlations indicate very different relationships between the times series and their shadow manifold predicted counterparts. Such information may be of interest and would be lost using only Δ (as defined above).

Another possible definition of the directed correlation comes from interpreting the pair (ρ_{XY}, ρ_{YX}) as a point in the unit square. To help keep things clear, the unit square in its specific use here will be referred to as the “directed correlation square” or “ D -square”. Points with no directed correlation (i.e. $\rho_{XY} = \rho_{YX}$) will fall along the diagonal bisector of the D -square that runs through the origin. Points with $\rho_{XY} > \rho_{YX}$ fall in the upper triangular area above the D -square bisector, and points with $\rho_{XY} < \rho_{YX}$ fall in the lower triangular area below the D -square bisector. Thus, the directed correlation can be determined from the location of the point (ρ_{XY}, ρ_{YX}) .

One of the most straightforward ways to quantify this concept is defining a 2-vector from the origin to the point (ρ_{XY}, ρ_{YX}) called \vec{D} . The magnitude of \vec{D} is

$$D_m = \sqrt{\rho_{XY}^2 + \rho_{YX}^2} ,$$

and its angle with the base of the D -square is

$$D_\theta = \arctan \left(\frac{\rho_{YX}}{\rho_{XY}} \right) .$$

(While it is possible for $\rho_{XY} = 0$ to occur and lead to the quotient in D_θ being undefined, such a point corresponds to a boundary point of the D -square where $D_\theta = \pi/2$ by definition.) A normalized angle can be defined as

$$D_{\theta n} = \frac{2}{\pi} \arctan \left(\frac{\rho_{YX}}{\rho_{XY}} \right) ,$$

which leads to “driving” rules similar to those mentioned for Δ at the beginning of this section (i.e. $D_{\theta n} < 1/2 \rightarrow "X \text{ drives } Y"$, $D_{\theta n} > 1/2 \rightarrow "Y \text{ drives } X"$, and $D_{\theta n} = 1/2$ indicates no directed correlation in the system).

The points used above lead to $D_{\theta n} \approx 0.4968$ (for $\rho_{XY} = 0.99$ and $\rho_{YX} = 0.98$) and $D_{\theta n} \approx 0.4423$ (for $\rho_{XY} = 0.06$ and $\rho_{YX} = 0.05$). Both Δ and $D_{\theta n}$ indicate that X “drives” Y but $D_{\theta n}$ also gives of more than just the differences of the CCM correlations. Naturally, there are pairs of CCM correlations that cannot be distinguished by $D_{\theta n}$. For example, $D_{\theta n} \approx 0.2952$ could result from either $\rho_{XY} = 0.88$ and $\rho_{YX} = 0.44$ or $\rho_{XY} = 0.44$ and $\rho_{YX} = 0.22$. Such points, however, would be distinguished by D_m (e.g. $D_m \approx 0.9839$ and $D_m \approx 0.4919$ for the examples points of the previous sentence).

A natural question would be why a pair of real numbers (both on the unit interval), i.e. (ρ_{XY}, ρ_{YX}) , should be replaced with a 2-vector on the unit square to define “directed correlation”. What are the benefits to defining “directed correlation” as a 2-vector rather than just a pair of CCM correlations? The biggest benefit is the use of geometric intuition in comparing different directed correlations. Overall, plotting the D -square will prove to be a quicker (and less confusing) way to present the directed correlation when compared to just calculating Δ .

For example, consider the example presented above. The first plot in the series of four plots is a scatter plot of the CCM correlation points (ρ_{XY}, ρ_{YX}) with individual histograms for ρ_{XY} and ρ_{YX} along the horizontal and vertical axis respectively. The second plot is a point density histogram of the points presented in the first plot. The last two plots are the directed correlation calculated with two separate averaging methods. “Mean method 1” refers to calculating the directed correlation as

$$\begin{aligned} |D| &= \sqrt{\langle X \rangle^2 + \langle Y \rangle^2} \\ D_\theta &= \arctan\left(\frac{\langle Y \rangle}{\langle X \rangle}\right) \end{aligned}$$

“Mean method 2” refers to calculating the directed correlation as

$$\begin{aligned} |D| &= \langle |D|_i \rangle \\ D_\theta &= \langle D_{\theta,i} \rangle \end{aligned}$$

with

$$\begin{aligned} |D|_i &= \sqrt{X_i^2 + Y_i^2} \\ D_{\theta,i} &= \arctan\left(\frac{Y_i}{X_i}\right) \end{aligned}$$

The two methods are not formally equivalent, but in practice, the difference is generally very small. The first averaging method is what is generally referred to as a “vector average” and as such will be the method used from here on. Both methods are presented below just for completeness. Notice that all of the plots agree with previous results (including the secondary peak about $\Delta = 0$ seen in the previous histograms) and intuition.

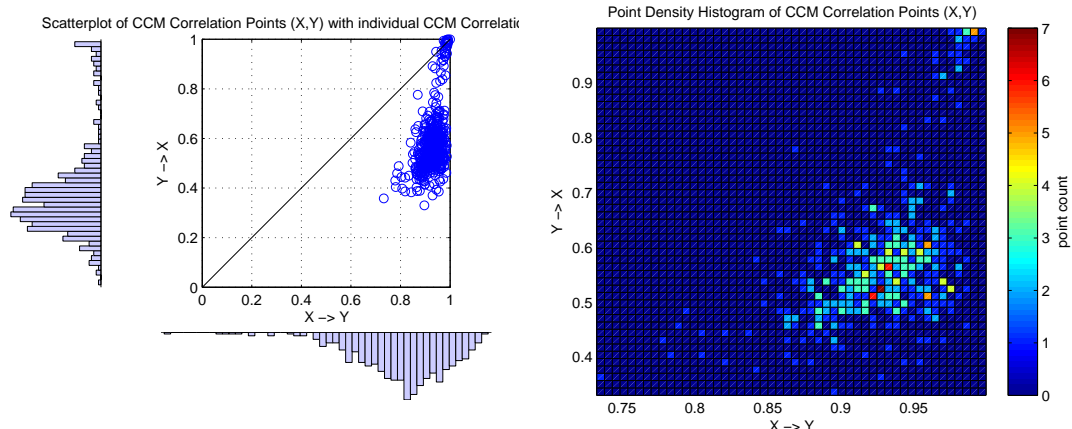
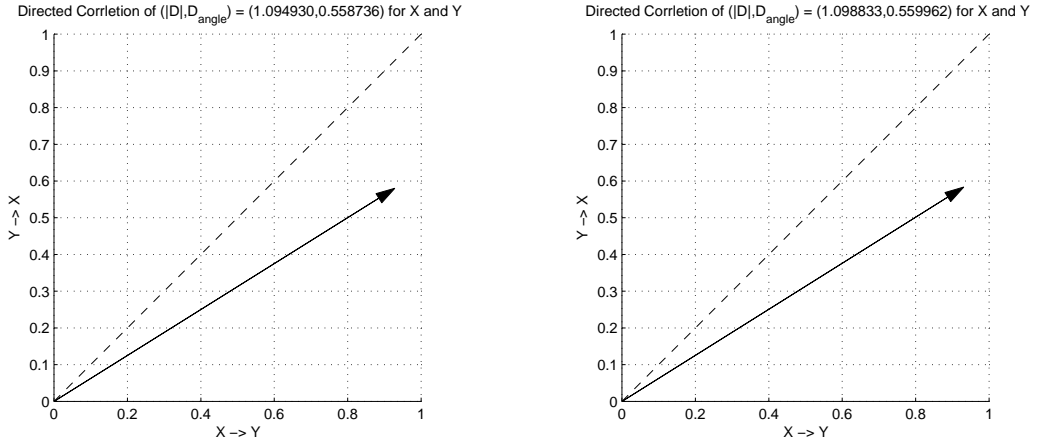


Figure 18

8 Applying CCM to Known Dynamics

The results shown above for the example presented by Sugihara appear to imply the following:

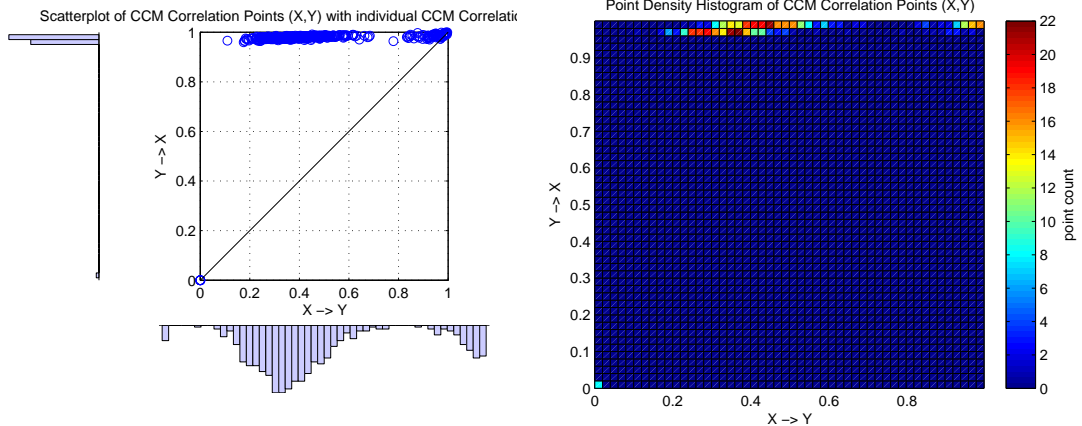
1. The CCM method is not robust with respect to the embedding dimension (i.e. E) or lag time step (i.e. τ).



(a) Mean Method 1: 500 samples with $(\mu_{rx}, \mu_{ry}, \sigma_{rx}^2, \sigma_{ry}^2, \mu_{x0}, \mu_{y0}, \sigma_{x0}^2, \sigma_{y0}^2) = (3.8, 3.5, 0.05, 0.05, 0.4, 0.2, 0.1, 0.1)$ and $(E, \tau) = (3, 1)$ for $L = 1000$ and $(\beta_{xy}, \beta_{yx}) = (0.02, 0.1)$.

(b) Mean Method 2: 500 samples with $= (\mu_{rx}, \mu_{ry}, \sigma_{rx}^2, \sigma_{ry}^2, \mu_{x0}, \mu_{y0}, \sigma_{x0}^2, \sigma_{y0}^2) = (3.8, 3.5, 0.05, 0.05, 0.4, 0.2, 0.1, 0.1)$ and $(E, \tau) = (3, 1)$ for $L = 1000$ and $(\beta_{xy}, \beta_{yx}) = (0.02, 0.1)$.

Figure 19



(a) 500 samples with $(\mu_{rx}, \mu_{ry}, \sigma_{rx}^2, \sigma_{ry}^2, \mu_{x0}, \mu_{y0}, \sigma_{x0}^2, \sigma_{y0}^2) = (3.1, 3.9, 0.05, 0.05, 0.4, 0.2, 0.1, 0.1)$ and $(E, \tau) = (3, 1)$ for $L = 1000$ and $(\beta_{xy}, \beta_{yx}) = (0.2, 0.002)$.

(b) 500 samples with $= (\mu_{rx}, \mu_{ry}, \sigma_{rx}^2, \sigma_{ry}^2, \mu_{x0}, \mu_{y0}, \sigma_{x0}^2, \sigma_{y0}^2) = (3.1, 3.9, 0.05, 0.05, 0.4, 0.2, 0.1, 0.1)$ and $(E, \tau) = (3, 1)$ for $L = 1000$ and $(\beta_{xy}, \beta_{yx}) = (0.2, 0.002)$.

Figure 20

2. The CCM method can lead to results that agree with intuition for the presented example.

These points will be explored by applying the CCM to two very different sets of dynamics. The first will explore a driven system by comparing the directed correlations calculated between the voltage and current time series of an RL circuit, and the second will explore the directed correlations found in the Lorenz system, which is known to be chaotic.

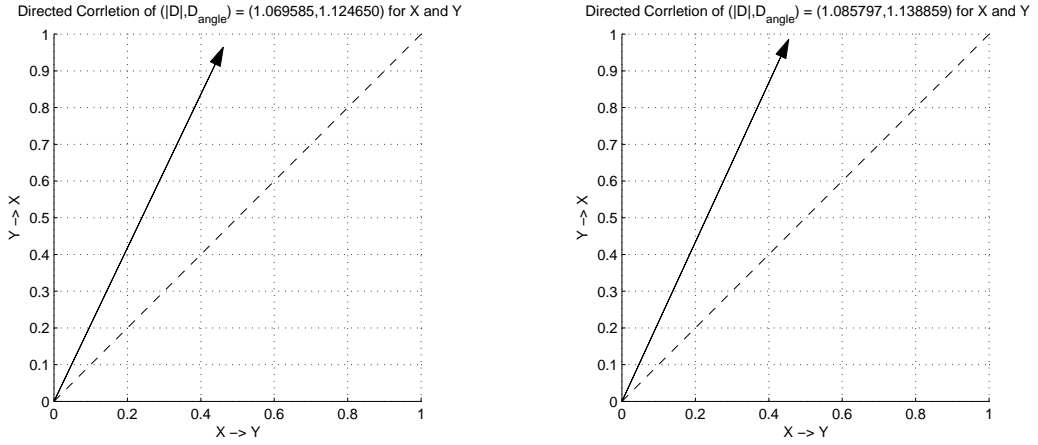
8.1 RL Circuit

An RL circuit is described as

$$\dot{I} = \frac{V}{L} - \frac{R}{L}I ,$$

where I is the current, V is the voltage, R is the resistance, and L is the inductance. The driving time series will be the voltage V and the response time series will be the current I . The resistance and inductance will be considered fixed.

Consider an RL circuit with $(R, L) = (0.5, 10)$. If the voltage times series V consists of two triangular pulses separated by constant spans of $V = 0$, then the current times series I will likewise have two maxima



(a) Mean Method 1: 500 samples with $(\mu_{rx}, \mu_{ry}, \sigma_{rx}^2, \sigma_{ry}^2, \mu_{x0}, \mu_{y0}, \sigma_{x0}^2, \sigma_{y0}^2) = (3.1, 3.9, 0.05, 0.05, 0.4, 0.2, 0.1, 0.1)$ and $(E, \tau) = (3, 1)$ for $L = 1000$ and $(\beta_{xy}, \beta_{yx}) = (0.2, 0.002)$. (b) Mean Method 2: 500 samples with $= (\mu_{rx}, \mu_{ry}, \sigma_{rx}^2, \sigma_{ry}^2, \mu_{x0}, \mu_{y0}, \sigma_{x0}^2, \sigma_{y0}^2) = (3.1, 3.9, 0.05, 0.05, 0.4, 0.2, 0.1, 0.1)$ and $(E, \tau) = (3, 1)$ for $L = 1000$ and $(\beta_{xy}, \beta_{yx}) = (0.2, 0.002)$.

Figure 21

as seen in Figure ???. The directed correlations C_{VI} and C_{IV} can be plotted as a function of the embedding dimension E to show that $C_{VI} > C_{IV}$ for $E = 2, 3, \dots, 10$. This plot is Figure ???. This result (i.e. that the

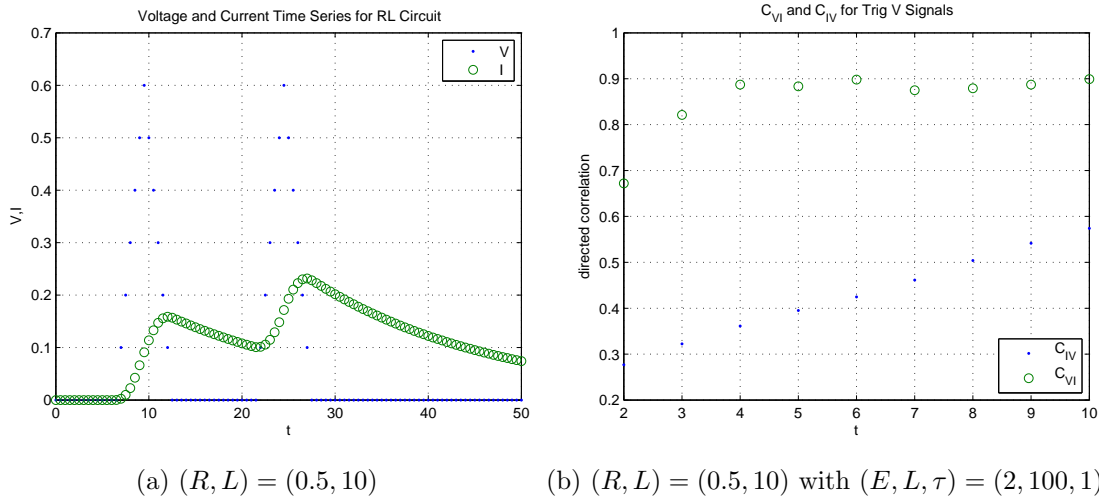


Figure 22

system is directionally correlated from V to I) is expected because $V \Rightarrow I$ (i.e. the voltage drives the current).

Consider the case when V is a discrete sine function; see Figure ?? for a plot of the V and I times series. The values of C_{VI} and C_{IV} are different than they were in the example of the previous paragraph but the general relationship is the same, i.e. $C_{VI} > C_{IV}$ for $E = 2, 3, \dots, 10$. See Figure ??.

The “non-robust” features of the directed correlations (with respect to E) can be recovered for the RL circuit by setting each point of V to be a random value. While such a voltage time series may be suspect (i.e. it results in possibly non-stationary current response time series), it will illustrate the same E -dependent behaviour of the directed correlations that was seen with the Sugihara example. Consider the V and I times series of Figure ??, where V is a set of pseudo-random numbers generated with Matlab. The plot of C_{VI} and C_{IV} for $E = 2, 3, \dots, 10$ (see Figure ??) shows that $C_{VI} > C_{IV}$ if $E \geq 4$ but $C_{VI} < C_{IV}$ if $E < 4$.

These results seem to imply that the robustness of the CCM method may be related to the autocorrelation of the “driving” time series. This idea will be explored after the next section.

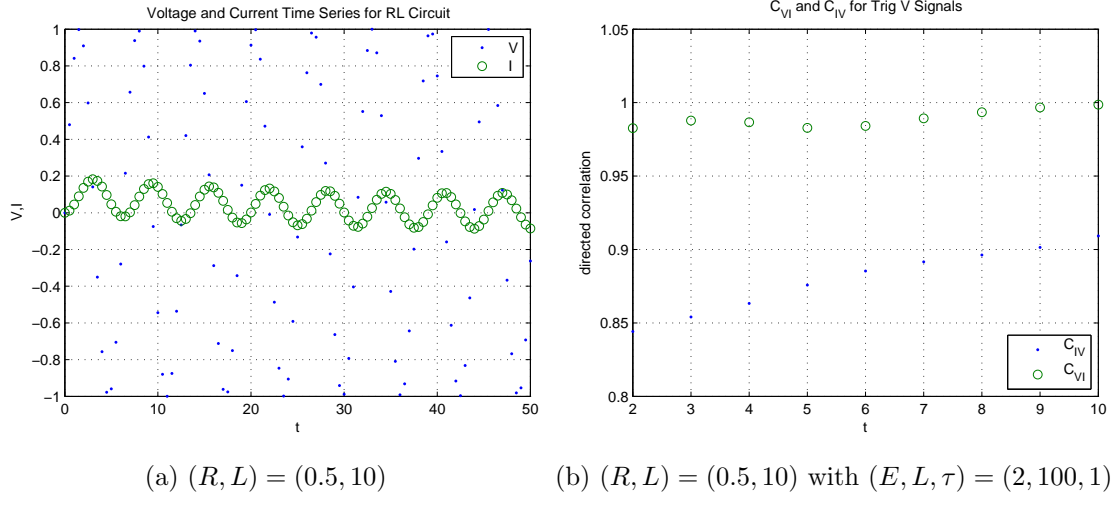


Figure 23

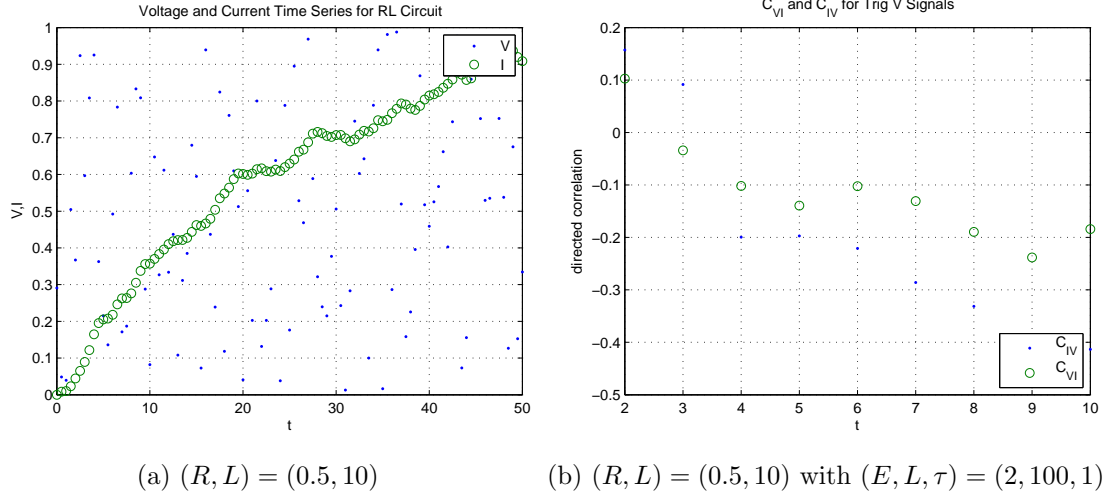


Figure 24

8.2 RL System with Voltage Dependent Resistance

Imagine the RL circuit is described above, i.e.

$$\dot{I} = \frac{V}{L} - \frac{R}{L}I ,$$

where I is the current, V is the voltage, R is the resistance, and L is the inductance, but with both V and R as time-dependent parameters. Consider, for example, that the resistance R is provided by a transistor⁷ or potentiometer. The driving time series will then be both the voltage V and the resistance R , and the response times series will still be the current I . Only the inductance will be considered fixed.

Suppose the voltage and resistance time series are given as pulses show in Figure ?? (which also shows the response I time series). The directed correlations between V and R , V and I , and I and R are shown in the Figure ???. These results imply that $V \rightarrow I$ and $R \rightarrow I$ with $V \rightarrow R$. These results agree with intuition.

Similar results are obtained if the voltage signal is

$$V(t) = \sin(t)$$

with a resistance of

$$R(t) = \sin(t) + 1.05 .$$

Those directed correlations are seen in Figure ???. Notice, however, that the directed correlation results are dependent on the phase of the resistance. Suppose the resistance is written down as

$$R(t) = A \sin(\omega t + \phi) + R_0 .$$

⁷<http://arxiv.org/ftp/arxiv/papers/0708/0708.3498.pdf>

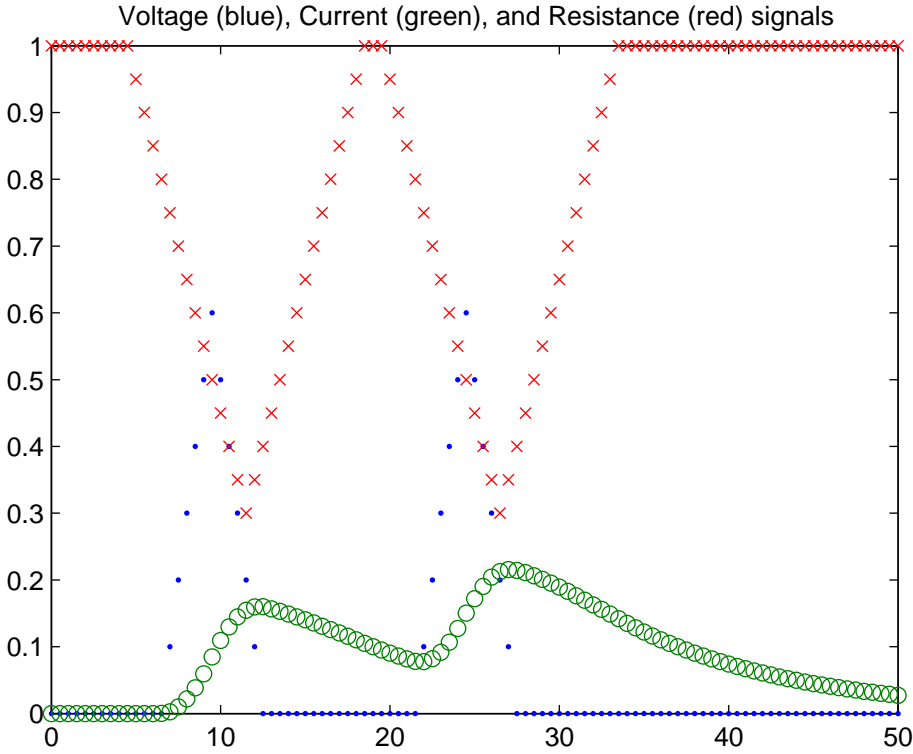
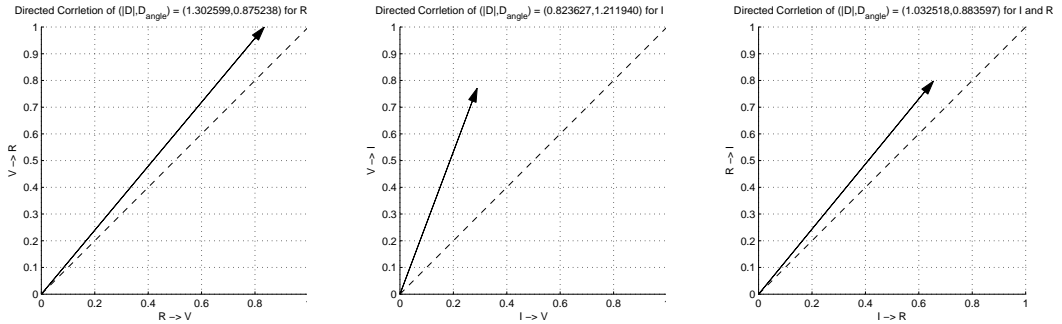


Figure 25: $L = 100$

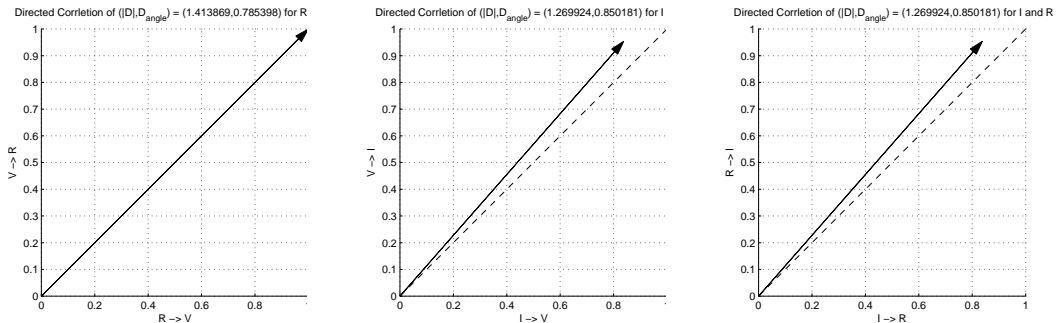


(a) $L = 100$ and V, R given in Figure ??.

(b) $L = 100$ and V, R given in Figure ??.

(c) $L = 100$ and V, R given in Figure ??.

Figure 26



(a) $L = 100$ and V, R given in text.

(b) $L = 100$ and V, R given in text.

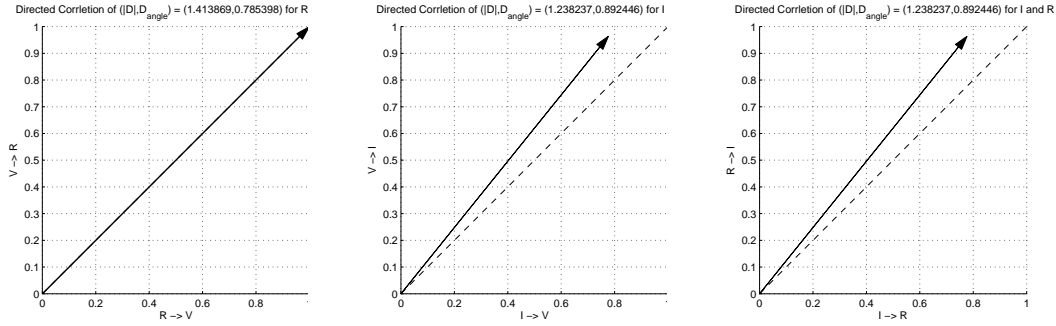
(c) $L = 100$ and V, R given in text.

Figure 27

The example above used $A = \omega = 1$, $R_0 = 1.05$ and $\phi = 0$, but notice that similar results (i.e. “intuitive results”) can be achieved even if $A \neq 1$, $R_0 \neq 1.05$ and $\phi \neq 0$.

Consider $A = R_0 = 0.5$ with $\omega = 1$ and $\phi = 0$. These values lead to the directed correlations in Figure ??.

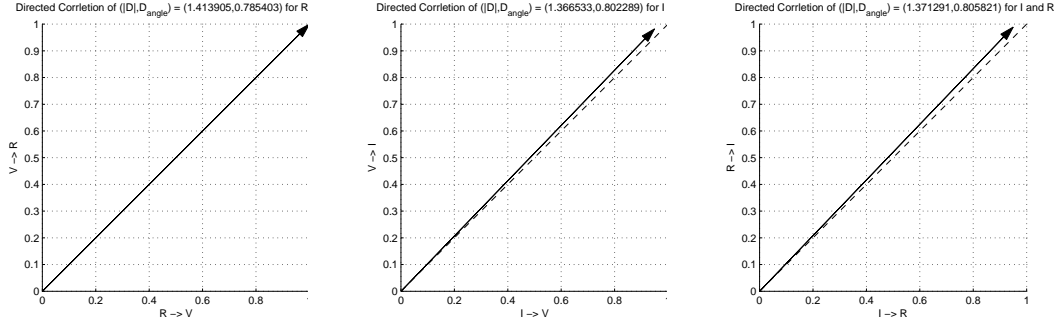
These results agree with what was seen in the previous examples.



(a) $L = 100$ and V, R given in text. $A = R_0 = 0.5$ with $\omega = 1$ and $\phi = 0$
(b) $L = 100$ and V, R given in text. $A = R_0 = 0.5$ with $\omega = 1$ and $\phi = 0$
(c) $L = 10$ and V, R given in text. $A = R_0 = 0.5$ with $\omega = 1$ and $\phi = 0$

Figure 28

Figure ?? shows the directed correlation when $A = \omega = 1$, $R_0 = 1.05$, and $\phi = \pi/2$. Again, these results

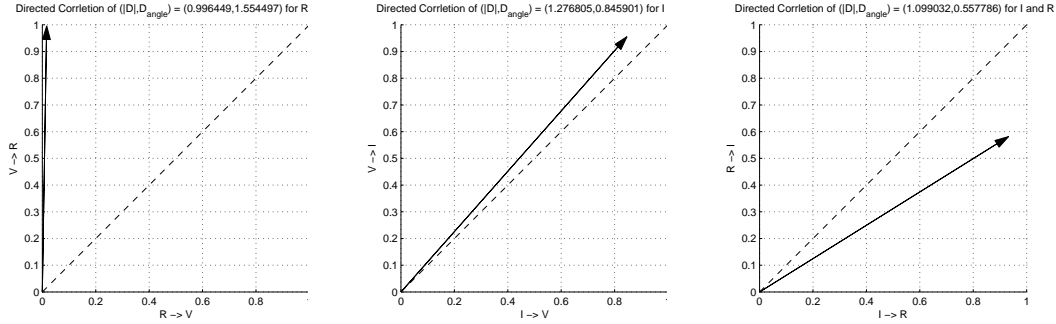


(a) $L = 100$ and V, R given in text. $A = \omega = 1$, $R_0 = 1.05$, $\phi = \pi/2$
(b) $L = 100$ and V, R given in text. $A = \omega = 1$, $R_0 = 1.05$, $\phi = \pi/2$
(c) $L = 100$ and V, R given in text. $A = \omega = 1$, $R_0 = 1.05$, $\phi = \pi/2$

Figure 29

agree with the previous results, although now the directed correlation between V and I is more different from the directed correlation between R and I than it was before.

Changing the phase ω , however, can lead to situations that do not support the intuitive result of $R \rightarrow I$. For example, consider $A = R_0 = \omega = 0.5$. These values lead to the directed correlations in Figure ???. These

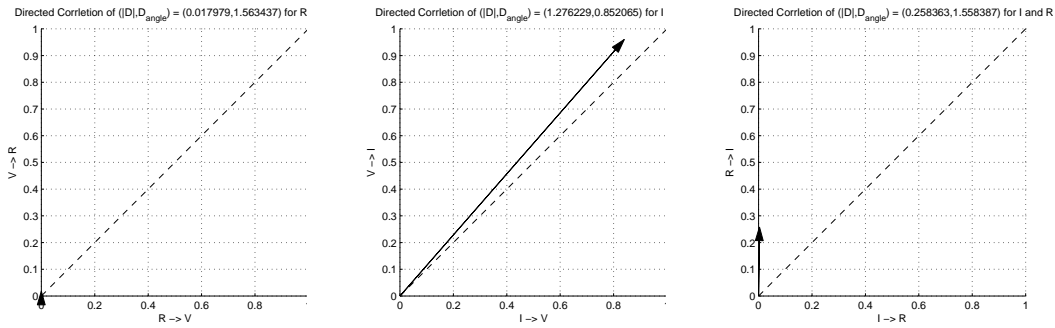


(a) $L = 100$ and V, R given in text. $A = R_0 = \omega = 0.5$
(b) $L = 100$ and V, R given in text. $A = R_0 = \omega = 0.5$
(c) $L = 100$ and V, R given in text. $A = R_0 = \omega = 0.5$

Figure 30

results imply $V \rightarrow I$, $I \rightarrow R$ and $V \rightarrow R$.

Consider the situation where the voltage is driven with the sinusoidal signal from above and the resistance is driven by the triangular pulse shown at the beginning of the section. Such a scenario leads to the directed correlations shown in Figure ???. These directed correlations imply $V \rightarrow I$ as expected, but it also implies $I \rightarrow R$



(a) $L = 100$ and V, R given in text. Triangular pulse R . (b) $L = 100$ and V, R given in text. Triangular pulse I . (c) $L = 10$ and V, R given in text. Triangular pulse R .

Figure 31

and $V \rightarrow R$ which apparently obeys transitivity (i.e. $V \rightarrow I$, $I \rightarrow R \Rightarrow V \rightarrow R$) but seems counter-intuitive as it was expected that $R \rightarrow I$.

The above results seem to imply that the voltage is the primary driver of the system and can, under certain scenarios, even be seen as a “driver” of the resistance through the current.

Consider approximating the above equation

$$\dot{I} = \frac{V}{L} - \frac{R}{L}I \Rightarrow I_{t+1} - I_t = \frac{V_t}{L} - \frac{R_t}{L}I_t .$$

Rearranging leads to

$$I_{t+1} = \frac{V_t}{L} + I_t \left(1 - \frac{R_t}{L} \right) ,$$

$$V_t = L \left(I_{t+1} - I_t \left(1 - \frac{R_t}{L} \right) \right) ,$$

and

$$R_t = L \left(I_t - I_{t+1} + \frac{V_t}{L} \right) .$$

These equations seem to imply that if the amplitude of the voltage is larger than both the resistance and the current, then the voltage will appear to drive both the current and the resistance. This is exactly the case seen in the above examples and points, again, to the problem of using language such as “driving” to describe the relationship indicated by the directed correlation. If the voltage, resistance, and current were all completely out of the experimenter’s control and the only data available is the time series described above. Then, it is reasonable that certain scenarios would allow the voltage to be used to predict both the resistance and the current because the voltage physically drives the current and shares a similar, repetitive mathematical structure with the resistance. The prediction ability of the voltage for the two quantities may come from different mechanisms (i.e. physical driving or mathematical structure), but the prediction ability itself is what is of interest to us here. This is what is meant by the term “driving”. It is not reasonable to state that the voltage physically drives the resistance in this particular case because by construction, the voltage and the resistance are independent. The voltage can “drive” the resistance in the sense that it can be used to predict the resistance. After writing all of this stuff, I’m starting to think that I should avoid using the term “driving” at all. Stick with the arrows and try to define it precisely at the beginning.

8.3 Three Population Example

Consider extending the two population model used by Sugihara et. al. to a “three population” model for $X(t)$, $Y(t)$, and $Z(t)$ defined as follows:

$$X_{t+1} = X_t (r_x - r_x X_t - B_{xy} Y_t - B_{xz} Z_t)$$

$$Y_{t+1} = Y_t (r_y - r_y Y_t - B_{yx} X_t - B_{yz} Z_t)$$

$$Z_{t+1} = Z_t (r_z - r_z Z_t - B_{zx} X_t - B_{zy} Y_t)$$

where all the parameters are non-negative real numbers.

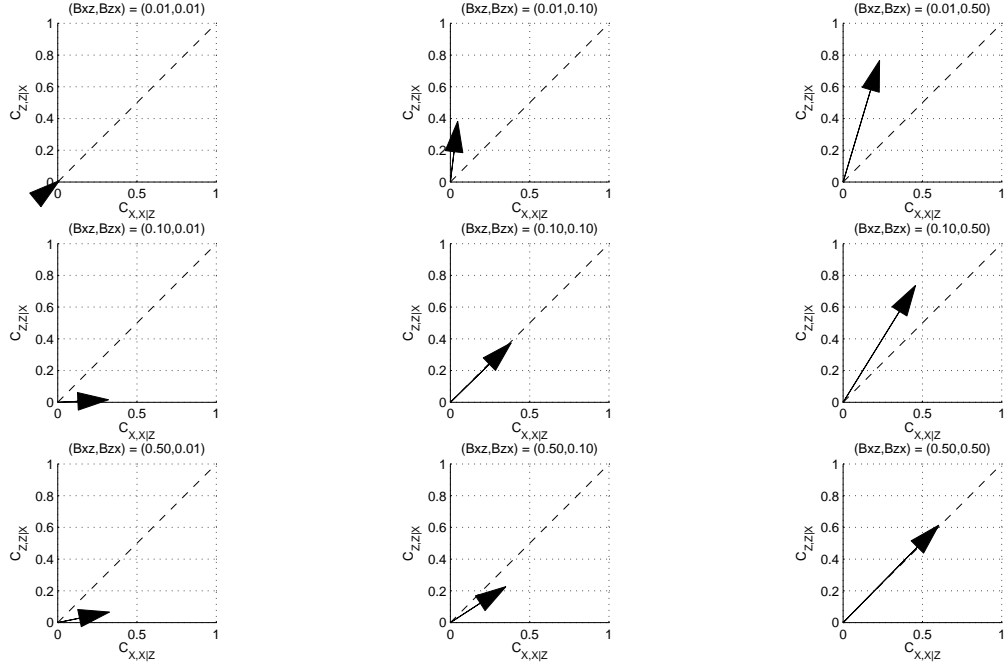


Figure 32: XZ and ZX plots.

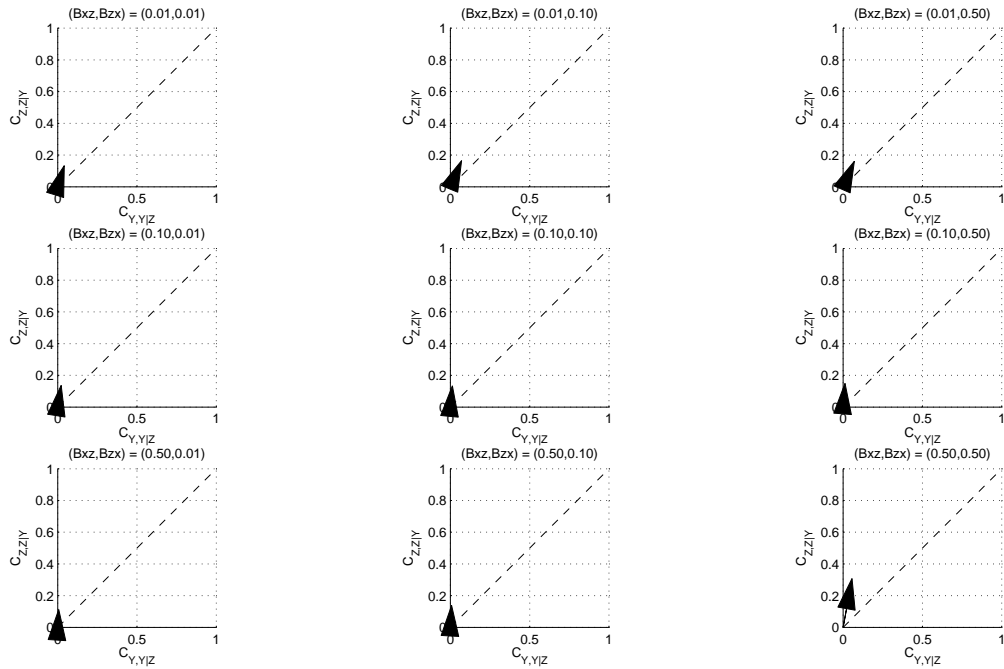


Figure 33: YZ and ZY plots.

8.4 Lorenz System

Consider the following system of equations:

$$\begin{aligned}\dot{x} &= \sigma(y - x) \\ \dot{y} &= \rho x - y - xz \\ \dot{z} &= xy - \beta z\end{aligned}$$

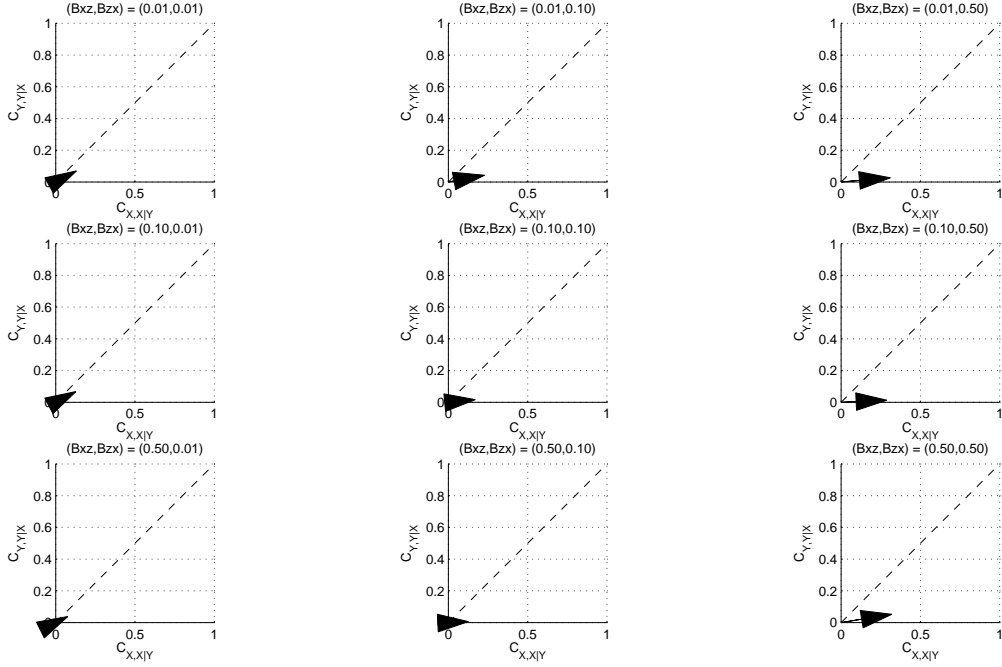


Figure 34: XY and YX plots.

If $(\sigma, \beta, \rho) = (10, 8/3, 28)$, then the system's directed correlations are as follows:

$$\begin{aligned} C_{xy} &\approx 0.91 \\ C_{yx} &\approx 0.94 \\ C_{xz} &\approx 0.11 \\ C_{zx} &\approx 0.88 \\ C_{yz} &\approx 0.08 \\ C_{zy} &\approx 0.45 \end{aligned}$$

where $x(t)$, $y(t)$, and $z(t)$ are defined by the dynamical system at the beginning of this section. These results seem to imply $z \Rightarrow x$ and $z \Rightarrow y$ with no conclusion for the relationship between x and y . These results seem confusing. In particular, it seems to make sense that z could be a stronger driver of y than y is of z (i.e. $z \Rightarrow y$) but the implication that z is a stronger driver of x than x is of z (i.e. $z \Rightarrow x$) is more difficult to interpret given that z only affects x through y .

If $(\sigma, \beta, \rho) = (0.01, 8/3, 28)$, then the system's directed correlations are as follows:

$$\begin{aligned} C_{xy} &\approx 0.79 \\ C_{yx} &\approx -0.12 \\ C_{xz} &\approx 0.90 \\ C_{zx} &\approx -0.74 \\ C_{yz} &\approx 0.47 \\ C_{zy} &\approx 0.71 \end{aligned}$$

which implies $x \Rightarrow y$, $z \Rightarrow y$, and $x \Rightarrow z$. Both $x \Rightarrow y$ and $x \Rightarrow z$ seems to make intuitive sense given the smaller σ in this example versus the previous example, and $z \Rightarrow y$ is consistent with the previous example which, again, makes sense because neither ρ nor β was changed.

If $(\sigma, \beta, \rho) = (10, 0.01, 28)$, then the system's directed correlations are as follows:

$$\begin{aligned} C_{xy} &\approx -1 \\ C_{yx} &\approx 1 \\ C_{xz} &\approx 0.02 \\ C_{zx} &\approx 0.30 \\ C_{yz} &\approx 0.01 \\ C_{zy} &\approx 0.40 \end{aligned}$$

This section will be expanded ...